울산대학교 공학연구논문집 제33권 1호 pp. 1~13, 울산대학교.
Journal of Engineering Research Vol. 33, No. 1, pp. 1~13, 2002
University of Ulsan.

A study on the exhaust airflow window system to reduce the space cooling load

Kim, Moo-Hyun · Kim, Dong-Lak
School of Mechanical and Automotive Engineering

<Astract>

The flow and heat transfer characteristics of a triple-glazed exhaust airflow window system were studied numerically by using the finite-volume method. Exhaust airfow rate, solar insolation and aspect ratio were considered important parameters. It was shown that space-heat gain was reduced considerably by increasing the exhaust airflow rate. Optimum exhaust airflow rate and aspect ratio were suggested to be Re = 600 and *W*/H = 0.05, respectively. Some comparisons between the airflow window system and the enclosed window system were made qualitatively and quantitatively.

실내 냉방부하절감을 위한 배기식 집열창시스템에 관한 연구

김무현 · 김동락
기계자동차공학부

<요 약>

하절기 냉방부하 절감 효과를 조사하고자 배기식 집열창시스템에 대해 유한체적법을 사용하여 수치해석적으로 연구하였다. 실내 공기를 시스템 내로 순환시킨 후 외부로 배출하는 모델을 선정하였고 배기공기유량, 태양열입사량 및 종횡비를 주요 변수로 고려하였다. 연구 결과에 의하면 배기공기량이 증가될수록 집열창으로 부터 실내로의 열취득이 현저히 감소되었다. 이때 주어진 태양열입사량에 대해 최적 배기공기량은 Re수로 약 600이었고 최적 종횡비는 대략 0.05이었다. 또한 여러가지 결과에 대해서 밀폐식집열창의 경우와 서로 비교하였다.

1. INTRODUCTION

It has been recognized that windows are thermally the weakest parts in the building envelope, increasing space heating and cooling load. Energy loss through windows amounts to over 3% of the total energy consumption of the United States [1, 3].

The number of studies concerning energy efficient building have increased in recent years. Research on highly thermal insulation problems of window systems has been conducted in many countries including the United States, Germany, Canada and Finland. These window systems, for example, are those with closed space filled with noble gases such as argon, krypton, and xenon [7, 14]; vacuum glazed windows [3, 4]; and coated low-emissive glazed windows [5]. These new window technologies, unfortunately, are often expensive and visibly uncomfortable. Window systems of energy-efficient buildings, however, should have two important qualities; low energy loss and high residential comfort.

Airflow window systems often provide these two factors, and thermal comfort. In general, double-glazed windows have an enclosed air layer between two glasses, while airflow windows have an open-air layer between two pieces of glass or between a glass and a solid wall, through which diverse flow patterns can exist. Thus the flow and thermal characteristics of airflow window systems are more complex and difficult. Air flow patterns between a glass and a roll screen were investigated to study thermal efficiency and effectiveness [13]. Many studies, mainly concerned with winter heating, were presented of airflow types between a glass and a wall (passive trombe wall) [2,6]. A study on a semi-open cavity with a screen and a siphon was conducted by Medved and Novak [10] to show how a screen provides good thermal insulation. There were numerous studies on double-glazed or double-pane window systems. However, few studies have been done on triple-glazed window systems. Theoretically, an enclosed triple-glazed window can reduce energy loss by about 1/3 more than an enclosed double-glazed window. Larsson *et al.* [8] recently investigated the thermal performance of an enclosed triple-glazed window system with low-emissivity coating and filled with krypton gas.

In this study, a numerical investigation is presented of a triple-glazed window with exhaust airflow through open-air layers. Three parameters; airflow rate, solar insolation and aspect ratio, are selected to study the impacts of parameters on the decrease in space-heat gain.

2. ANALYTICAL MODEL

A triple-glazed window system is shown in Figure 1. The window system is of height H and width W, and the Cartesian coordinates with the corresponding velocity

components(u,v) are indicated therein. This system has two open-air spaces; outer and inner air space, and three glazings; outer, middle and inner glazing. Indoors air flows through the inlet clearance at the top of the inner glazing, and exits through the outlet clearance.

This study considers the problems of mixed convections due to the combination of the buoyancy effect and the inlet/outlet flows. The physical model for the numerical calculation does not include any frame. That is, only the air spaces and solid glasses are calculated. The computational domain includes both fluid layers and solid layers, presenting what is here a conjugate problem. In this study, glazing is assumed to be a heat source which absorbs a portion of solar energy and then emits part of that energy.

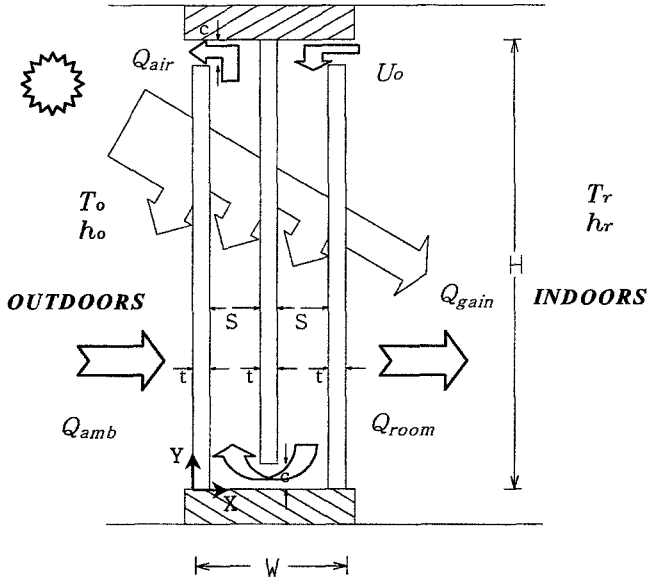

Figure 1. Schematic of an exhaust triple-glazed airflow window

3. MATHEMATICAL FORMULATION

3.1 Governing equations

The flow is assumed to be steady, laminar, incompressible and two-dimensional. Viscous dissipation is neglected and properties of the fluid are assumed to be constant except for the buoyancy term of the y-momentum equation, i.e., the Boussinesq approximation. The equations are obtained in dimensionless forms as follows:

$$\frac{\partial u}{\partial x}+\frac{\partial v}{\partial y}=0 \tag{1}$$

$$u\frac{\partial u}{\partial x}+v\frac{\partial u}{\partial y}=-\frac{\partial p}{\partial x}+\frac{V^{*}\sigma}{Re}\left(\frac{\partial^{2}u}{\partial x}+\frac{\partial^{2}u}{\partial y^{2}}\right) \tag{2}$$

$$u\frac{\partial v}{\partial x}+v\frac{\partial v}{\partial y}=-\frac{\partial p}{\partial y}+\frac{V^{*}\sigma}{Re}\left(\frac{\partial^{2}v}{\partial x^{2}}+\frac{\partial^{2}v}{\partial y^{2}}\right)+\frac{GR\sigma^{2}}{Re^{2}}\theta[1-f(\Omega)] \tag{3}$$

$$u\frac{\partial \theta}{\partial x}+v\frac{\partial \theta}{\partial y}=\frac{K^{*}\sigma}{PeC^{*}}\left(\frac{\partial^{2}\theta}{\partial x^{2}}+\frac{\partial^{2}\theta}{\partial y^{2}}\right)+\frac{Ns\,\sigma}{PeC^{*}}f(\Omega) \tag{4}$$

These equations were nondimensionalized by nondimensional variables as,

$$x=\frac{X}{H},\ y=\frac{Y}{H},\ u=\frac{U}{U_0},\ v=\frac{V}{U_0}\ p=\frac{P}{\rho {U_0}^{2}},\ \theta=\frac{T-T_r}{T_0-T_r},$$

$$Re=U_0\frac{(2c)}{v_f},\ \mathrm{Pr}=\frac{v_f}{a_f},\ Gr=\frac{g\beta(T_0-T_r)H^{3}}{{v_f}^{2}},\ Pe=Re\cdot \mathrm{Pr}, \tag{5}$$

$$Ns=\frac{q\cdot H^{2}}{k_f(T_0-T_r)},\ \sigma=\frac{2c}{H},\ k^{*}=\frac{k}{k_f},\ C^{*}=\frac{(\rho C_p)}{(\rho C_p)_f},\ v^{*}=\frac{v}{v_f}$$

where v^{*}, k^{*}, C^{*} are dimensionless kinematic viscosity, thermal conductivity and thermal capacitance, respectively. All of them are 1 at fluid region. At solid region, however, $v=v_s$, $k=k_s$, $(\rho C_p)=(\rho C_p)_s$ and dimensionless kinematic viscosity, $v^{*}(=v_s/v_f)$ is large enough to be 105 or 106, so that it is treated as solid in numerical calculations. $f(\Omega)$ is a step function with 0 at fluid region (air spaces) and with 1 at solid region (panes).

3.2 Boundary conditions

The appropriate velocity, temperature and solid-fluid interface boundary conditions are as follows:

* Velocity boundary conditions:

$u=0,\ v=0$	at Y=0, H	
$u=0,\ v=0$	at pane surfaces	(6)
$u=-1$	at air inlet and outlet clearances	

* Temperature boundary conditions:

$$\frac{\partial \theta}{\partial y} = 0 \qquad \text{at} \quad Y=0,\ H$$

$$\frac{Nu_r}{k^*}\theta_s = -\frac{\partial \theta_s}{\partial x} \qquad \text{at} \quad X = W \tag{7}$$

$$\frac{Nu_0}{k^*}(\theta_s - 1) = \frac{\partial \theta_s}{\partial x} \qquad \text{at} \quad X=0$$

$$\theta = 0 \qquad \text{at} \quad \text{air inlet clearance}$$

where Nu_r and Nu_o are Nusselt numbers calculated at the inside surface of the inner pane, and at the outside surface of the outer pane, respectively. These are given by

$$Nu_r = \frac{h_r H}{k_f}, \quad Nu_0 = \frac{h_0 H}{k_f} \tag{8}$$

* Fluid-solid interface conditions:

$$\theta_f = \theta_s, \quad k_f \frac{\partial \theta_f}{\partial n} = k_s \frac{\partial \theta_s}{\partial n} \tag{9}$$

where **n** is a unit vecror at solid-fluid interface.

3.3 Energy balance

An energy balance is obtained as follows for the control volume of window system:

$$Q_{gain} + Q_{amb} + Q_{room} + Q_{air} = 0 \tag{10}$$

where Q_{gain} is the portion of solar energy absorpted by panes, Q_{amb} is the efflux energy transfered to the outdoor through the outer pane, Q_{room} is the influx energy transfered to the indoor through the inner pane, and Q_{air} is the energy transported by air mass flow rate. Q_{room} means the room- or space-heat gain through the inner pane, which results in the increase of space cooling load in summer. Equation (10) can also be transformed into

$$(Q_{amb} + Q_{room} + Q_{air}) \ / \ Q_{gain} = -1 \tag{11}$$

and equation (11) is used to confirm the validity of the analytical model and its computation presented here. Each term of equation (10) can be caculated as follows:

$$
\begin{aligned}
Q_{gain} &= (q_1+q_2+q_3)A \cdot t \\
Q_{amb} &= h_0 \cdot A(T_0 - T \mid_{x=0}) \\
Q_{room} &= -h_r \cdot A(T \mid_{x=w} - T_r) \\
Q_{air} &= -mC_p[T_{out,b} - T_r]
\end{aligned}
\tag{12}
$$

In equation (12) q_1, q_2, and q_3 are absorbed heat per unit volume by three panes, and are given as

$$
q_1 = (I/t) \cdot A_{3(1)}, \quad q_2 = (I/t)A_{3(2)}, \quad q_3 = (I/t)A_{3(3)} \tag{13}
$$

where $A_{3(1)}$, $A_{3(2)}$, $A_{3(3)}$ are absorptivities of outer, middle and inner pane, respectively, which can be calculated using the Net Radiation Method [12]. The external convective heat transfer coefficient, h_o, and the internal convective heat transfer coefficient, h_r, are calculated from the relationships suggested by Lokmanhekin and McAdams [9], apart. They yield

$$
\begin{aligned}
h_0 &= 8.07\,V^{0.605}[W/m^{2o}C], \; V_\infty > 2.0m/s \\
h_r &= 1.42(\triangle T/H)^{1/4}[W/m^{2o}C]
\end{aligned}
\tag{14}
$$

3.4 Calculation procedure

The governing equations are solved using the finite volume method by Patankar [11]. A grid system of 40×110 nodes is used for basic calculation. The relaxation factors are 0.7, 0.3, and 0.4 for energy equation, momentum equation, and pressure-correction equation, repectively. The number of iteration is about 1,500-4,000, and the criterion for numerical convergence, i.e., the maximum relative difference between two consecutive iterations, is less than 10^{-6}. The properties of the air and glass and the specifications of the window system are given in Tables Ⅰ and Ⅱ.

Table Ⅰ. Properties of glass and air

Properties	Glass	Air
Conductivity, k (W m^{-1} K^{-1})	0.756	0.025
Density, (kg m^{-3})	2550	1.165
Specific Heat, C_p (J kg^{-1} K^{-1})	754	1006
Kinematic Viscosity, ν(m^2 s^{-1})	-	1.5×10^{-5}
Prandl Number, Pr	-	0.70
Absorptivity, A	0.139	-
Reflectivity, R	0.072	-
Transmissivity, T	0.789	-

Table II. Specifications of the exhaust airflow window system (unit;m)

Aspect Ratio, *W*/H	Width, *W*	Height, H	Thickness, t	Clearance, *c*	Width, S
0.03	0.027	0.900	0.006	0.005	0.0045
0.04	0.036	0.900	0.006	0.005	0.0090
0.05	0.045	0.900	0.006	0.005	0.013
0.10	0.090	0.900	0.006	0.005	0.0360

4. RESULTS AND DISCUSSIONS

4.1 Characteristics of energy balance

To provide an insight into the energy balance characteristics of the system with increasing Reynolds number, dimensionless forms of the calculated energies, Q/Q_{gain}, are given in Figure 2. In the figure, Reynolds number implies the flow rate of exhaust air through the air spaces. Re = 0, therefore, also implies the case of enclosed windows. The minus sign (-) means the energy efflux from the control volume to the surrounding area, while plus sign (+) means the energy influx from the surrounding area to the control volume.

From Figure 2, the relation of energy balance, eq. (11) is clear, which means that the numerical calculations presented here are valid within the range of variables. For increasing Reynolds numbers, Q_{air}/Q_{gain} becomes absolutely larger, which represents the energy flows out to the surrounding area by convection flow. Room-heat gain (or space-heat gain), Q_{room}/Q_{gain}, however, becomes smaller and smaller to approach zero as the Reynolds number increases. It is worth noting that in the summer space-heat gain can be reduced considerably by increasing the exhaust air flow rate. Some discussion of the optimum value of exhaust air flow rate will be presented later. Q_{amb}/Q_{gain}, the energy transfered outdoors, shows the heat efflux through the outer pane at Re = 0, and shows the heat influx through the outer pane at Re $\geq$ 200.

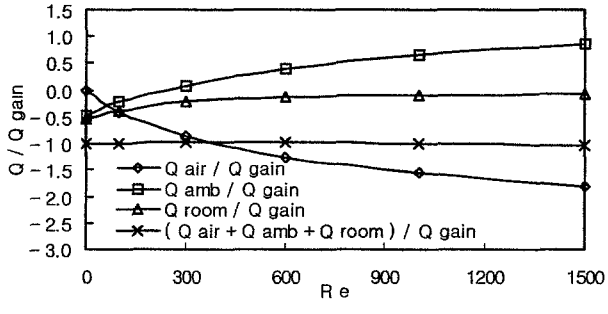

Figure 2. Calculated heat rates for various Reynolds numbers with I_t = 600 W/m^2

4.2 Effects of solar insolation

In order to investigate the effects of the solar insolation on the flow and temperature fields, global views of the streamline and isotherm for the exhaust and the enclosed windows are shown in Figure 3. In the case of the exhaust windows with Re = 300, Figure 3(a), a clockwise cell is observed both at the lower part of the outer air space and at the upper part of the inner air space. As the solar insolation increases, intensity of the cell, appearing at the upper part of the inner air space, increases due to the increase in the buoyancy effect.

In the case of the enclosed window with Re = 0, Figure 3(b), two cells in the outer air layer and unicell in the inner air layer appear for I_t = 100W/m^2. For the increasing solar intensity to be 400 and 600W/m^2, however, unicell appears in each air layer. Therein, the unicell observed in the outer layer flows counter-clockwise, while the unicell observed in the inner layer flows clockwise, because the middle pane has a relatively higher temperature than the others.

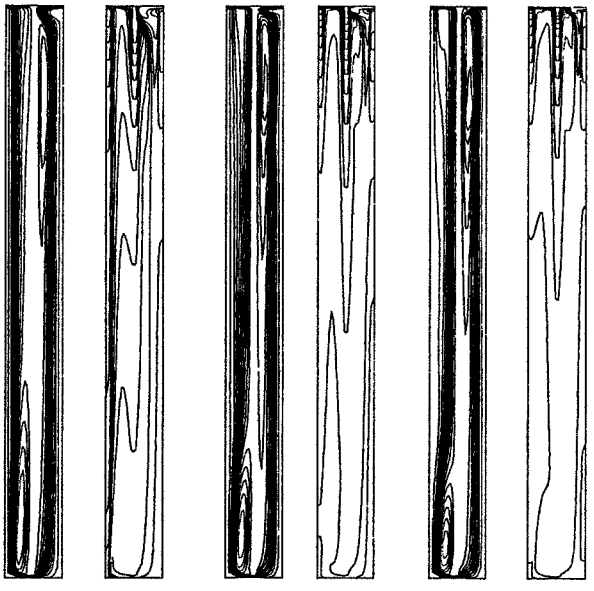

(a) Exhaust airflow window

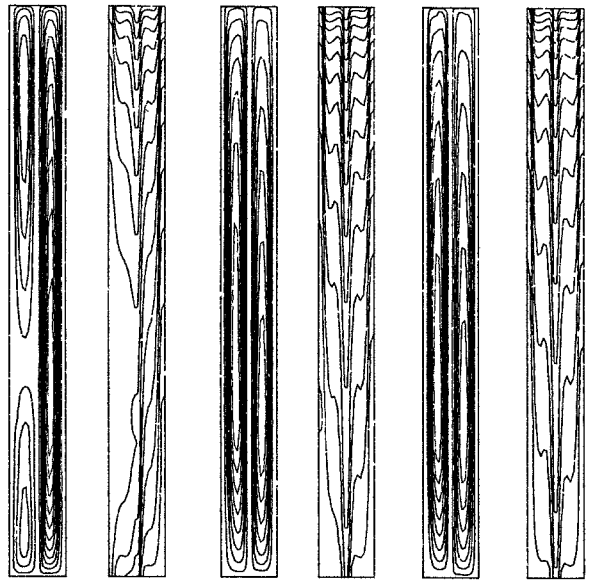

$I_t = 100W/m^2$ $I_t = 400W/m^2$ $I_t = 600W/m^2$

(b) Enclosed window

Figure 3. Effect of solar insolation on the streamlines and isotherms with W/H = 0.1 and Re = 300

4.3 Effects of exhaust airflow rate

The exhaust air flow rate through the air spaces is the most important variable in the present parametric study. Figure 4 shows the variations of the room-heat gain, Q_{room}, for the increasing Reynolds number, and I_t = 600W/m^2. First of all, it can be seen that space-heat gain, Q_{room}, is remarkably reduced with increasing Reynolds numbers, i.e., the exhaust air flow rate. Now, effects of the exhaust air flow rate on the space-heat gain are investigated in detail.

For Re = 0, i.e., no exhaust air flow, the space-heat gains are about 75W for four aspect ratios. The space-heat gains, however, decrease in nearly exponential pattern as Reynolds numbers increase. The decrements in space-heat gains are considerably larger in the range of low Reynolds numbers, but are relatively small in the range of Re$\geq$600. Consequently, the optimum value of the exhaust air flow rate discussed earlier appears to be Re $\fallingdotseq$ 600. For Re = 600 and W/H = 0.05, space-heat gain is

about 30W, which corresponds to 40% of that of enclosed windows. In other words, this results in a 60% decrease compared to the case of enclosed windows.

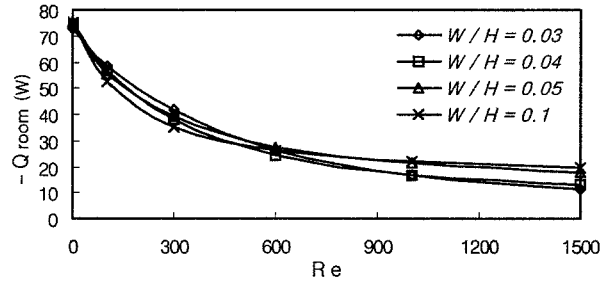

Figure 4. Effect of Reynolds number on the space-heat gain for I_t = 600 W/m^2

4.4 Effects of aspect ratio

Under an identical physical situation, changes in the aspect ratio, *W*/H, vary the space-heat gain. Numerical results for four aspect ratios and I_t = 100W/m^2 are presented in Figure 5. As shown in the figure, the effect of the aspect ratio on the space-heat gain is negligible in the range of Re>600. However, it is important in the range of Re≤600. It can be seen that for a Reynolds number (for example, Re = 300), the decrease in the space-heat gain becomes evident with an increasing aspect ratio in the range of *W*/H≤0.05. However, it is not obvious in the range of *W*/H>0.05. This suggests that the value of the aspect ratio, *W*/H ≒ 0.05, is appropriate for the optimum value in the present numerical analysis.

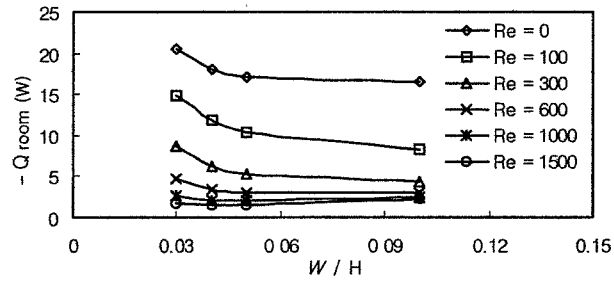

Figure 5. Effect of aspect ratio on the space heat gain for I_t = 100 W/m^2

5. CONCLUSIONS

A numerical study for a triple-glazed air flow window model has been conducted parametrically to show the effects of solar insolation, exhaust airflow rate, and aspect

ratio on the decrease in space-heat gain, which stands for the decrease in space cooling load. The results obtained here are compared with those of an enclosed window system.

For the air flow windows with I_t = 100, 400 and 600W/m^2, a clockwise cell is observed both at the lower part of the outer air space and at the upper part of the inner air space. With increasing solar insolation, the intensity of the cell appearing at the upper part of the inner air space increases due to an increase in the buoyancy effect. The space-heat gain decreases in a nearly exponential pattern as Reynolds numbers increase. The decrements in space heat-gains are considerably larger in the range of low Reynolds numbers, but are relatively small in the range of Re≥600. The optimum value of the exhaust air flow rate is suggested to be Re ≒ 600. For Re = 600 and W/H = 0.05, space heat-gain is about 30W, which corresponds to 40% of that of enclosed windows. This results in a 60% decrease from the case of enclosed windows. It is also suggested that the value of the aspect ratio, W/H ≒ 0.05, is appropriate for the optimum value in the present numerical analysis.

NOMENCLATURE

A = area of glazing (m^2)
A = absorptivity of glazing
c = clearance (m)
C = heat capacity (kJ m^{-3} K^{-1})
C_p = specific heat (kJ kg^{-1} K^{-1})
g = gravitational acceleration (m s^{-2})
Gr = Grashof number
h = convective heat transfer coefficient (W m^{-2} K^{-1})
H = height of the window (m)
I_t = solar insolation per unit area (W m^{-2})
k = thermal conductivity (W m-1 K^{-1})
m = exhaust air mass flowrate (kg s^{-1})
n = unit vector
Ns = nondimensional number on heat absorption by panes
Nu = Nusselt number
P = pressure (kPa)
p = nondimensional pressure
Pe = Peclet number

Pr = Prandtl number
q = absorbed energy per unit volume (W m^{-3})
R = reflectivity of glazing
Re = Reynolds number
S = width between panes (m)
t = thickness of glazing (m)
T = transmissiviy of glazing
T = temperature (K)
$T_{out,b}$ = bulk temperature at the outlet (K)
U, V = velocites of the x- and y-direction (m s^{-1})
V_∞ = velocity of outdoor air (m s^{-1})
u, v = dimensionless velocities of the x- and y-direction
W = width of the window (m)
X, Y = x- and y-coordinate (m)
x, y = dimensionless x- and y-coordinate

Greek symbols

α = thermal diffusivity (m^2 s^{-1})
β = thermal expansion coefficient (K^{-1})
θ = dimensionless temperature
v = kinematic viscosity (m^2 s^{-1})
σ = nondimensional clearance
ρ = density (kg m^{-3})

Subscripts

* = dimensionless value
1,2,3 = outer, middle, inner pane
f = *fluid*
o = *outdoor*
r = room/indoor
s = solid

* This work was supported by the University of Ulsan Research Fund of 2000

REFERENCES

1. Arasteh D, Selkowitz S, Wolfe JR. 1989. The design and testing of a highly insulating glazing system for use with conventional window systems. *Journal of Solar Energy Engineering.* **111**: 44-53.
2. Barozzi GS, Ibabi MSE, Nobile E, Sousa ACM. 1992. Physical and numerical modeling of a solar chimney-based ventilation system for building. *Building and Environment* **27**: 433-441.
3. Collins RE, Turner GM, Fisch-Cripps AE, Tang JZ. 1995. Vacuum glazing - a new component for insulating windows. *Building and Environment* **30**: 459-492.
4. Collins RE, Davis CA, Dey CJ, Robinson SJ, Tang JZ, Turner GM. 1993. Measurement of local heat flow in flat evacuated glazing. Int. J. of Heat Mass Transfer **36**: 2550-2563
5. Elmahdy AH, Comick SM. New technology in the window industry. *Building Science Insight* **88**.
6. Gan G. 1998. A parametric study of trombe walls for passive cooling of buildings. *Energy and Buildings* **27**: 37-43.
7. Hanley HJM, McCarty RD, Haynes WM. 1974. The viscosity and thermal conductivity coefficients for dense gaseous and liquid argon, krypton, xenon, nitrogen and oxygen. *J. Phys. Chem. Ref. Data.* **3**(4) : 979-1018.
8. Larsson U, Moshfegh B, Snadberg M. 1999. Thermal analysis of super insulated windows (numerical and experimental investigations). *Energy and Buildings* **29**: 121-128.
9. McAdams WH. 1954. Heat Transmission, 3rd edtion, *McGraw-Hill*:New York.
10. Medved S, Novak P. 1998. Heat transfer through a double pane window with an insulation screen open at the top. *Energy and Buildings* **28**: 257-268.
11. Patankar SV. 1980. Numerical Heat Transfer and Fluid Flow, *McGraw-Hill*: New York.
12. Siegel R, Howell JR. 1972. Thermal Radiation Heat Transfer. *McGraw Hill*: New York.
13. Tanimoto J, Kimura K. 1997. Simulation study on an air flow window system with and integrated roll screen. *Energy and Buildings* **26**: 317-325.
14. Weir G, Muneer T. 1998. Energy and Environmental Impact Analysis of Double-Glazed Windows. *Energy Convers. Manage.* **39**: 243-256.